Real Time Green's Functions from NCA based Impurity Solver

Tel Aviv University

9/02/2018

Introduction

Strongly correlated materials.

- Idea of description of electrons in solids as independent particles
  $\rightarrow$ wave-like picture
- Materials in which electrons tend to *localize*
  $\rightarrow$particle-like picture
- Strong electronic correlations brings out a variety of phenomena, e.g. metal-to-Mott-insulator transitions

Description of the lattice

Hubbard model.

$$H_{\text{Hubbard}} = -\sum_{\langle i,j\rangle,\sigma} v_{ij} d^{\dagger}_{i\sigma} d_{j\sigma} + \sum_{i} U(d^{\dagger}_{i\uparrow} d_{i\uparrow} - \frac{1}{2})(d^{\dagger}_{i\downarrow} d_{i\downarrow} - \frac{1}{2})$$

- $v_{ij} \simeq$ overlap between orbitals on neighbouring atomic sites $\sim$ eV
- Coulomb repulsion U, screened value $\sim$ eV

  $\rightarrow$ competition between energy scales

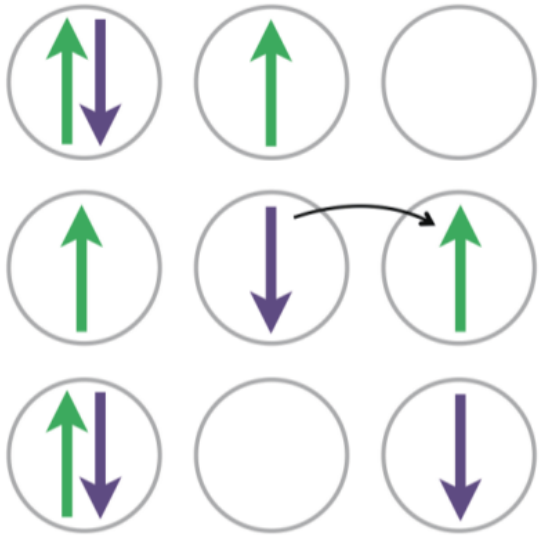

Figure 1: Lattice model

source: H. Aoki, N. Tsuji, M. Eckstein, M. Kollar, T. Oka, and P. Werner, Rev. Mod. Phys. 86, 779 (2014)

Dynamical Mean Field Theory

Idea of mapping.

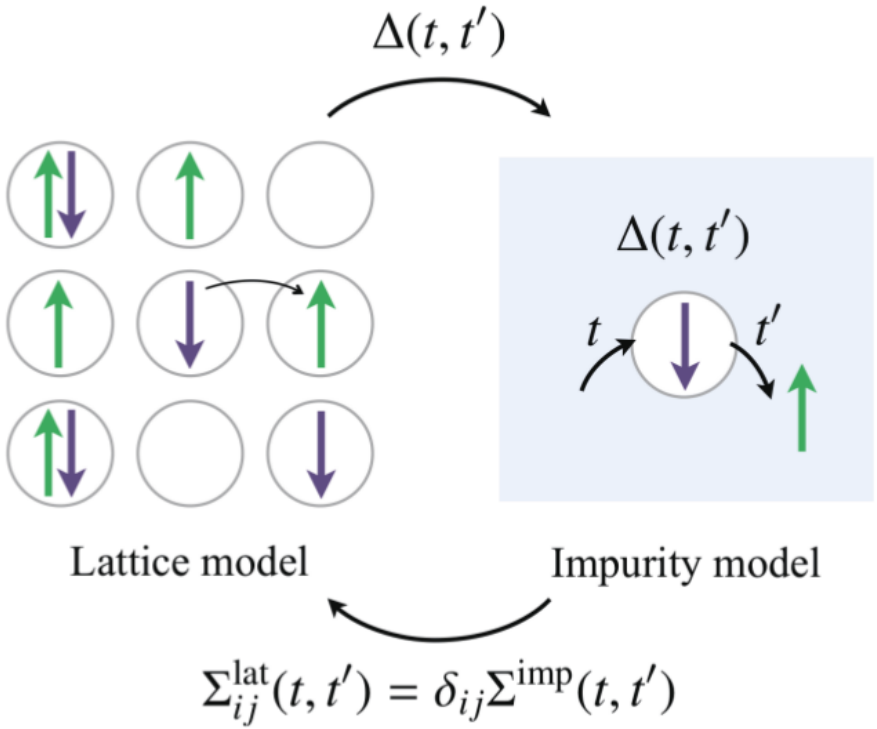

Figure 2: Mapping of the lattice problem onto an Impurity problem

- Approximate lattice problem with many degrees of freedom by *single-site problem*

Dynamical Mean Field Theory

Set of self-consistent equations.

- compute local Greens function $G_{ii}^{\sigma}(t-t') = -i\langle \mathscr{T} d_{i\sigma}(t) d_{i\sigma}^{\dagger}(t')\rangle$ from an effective impurity model with action

$$S = i\int_C dt U n_{\uparrow}(t) n_{\downarrow}(t) - i\sum_{\sigma}\int_C dt dt' d_{\sigma}^{\dagger}(t)\Delta(t-t') d_{\sigma}(t')$$

- use impurity self energy, defined via $G_{ii}^{-1}(\omega) = \omega + \mu - \Delta(\omega) - \Sigma^{imp}(\omega)$, to obtain the lattice Greens function

$$G_{ij}^{-1}(\omega) = \delta_{ij}[\omega + \mu - \Sigma_{ii}(\omega)] - v_{ij}$$

$$\Sigma_{ii}(\omega) \simeq \Sigma^{imp}(\omega); \Sigma_{i\neq j}(\omega) \simeq 0$$

- average over the Brillouin zone to get the on-site component:

$$G_{ii}(\omega) = \frac{1}{L}\sum_k G_k(\omega) = \frac{1}{L}\sum_k \frac{1}{\omega + \mu + \Sigma(\omega) - \varepsilon_k}$$

Dynamical Mean Field Theory

Set of self-consistent equations.

$$\mathcal{G}_0 = \omega + \mu - \Delta(\omega)$$

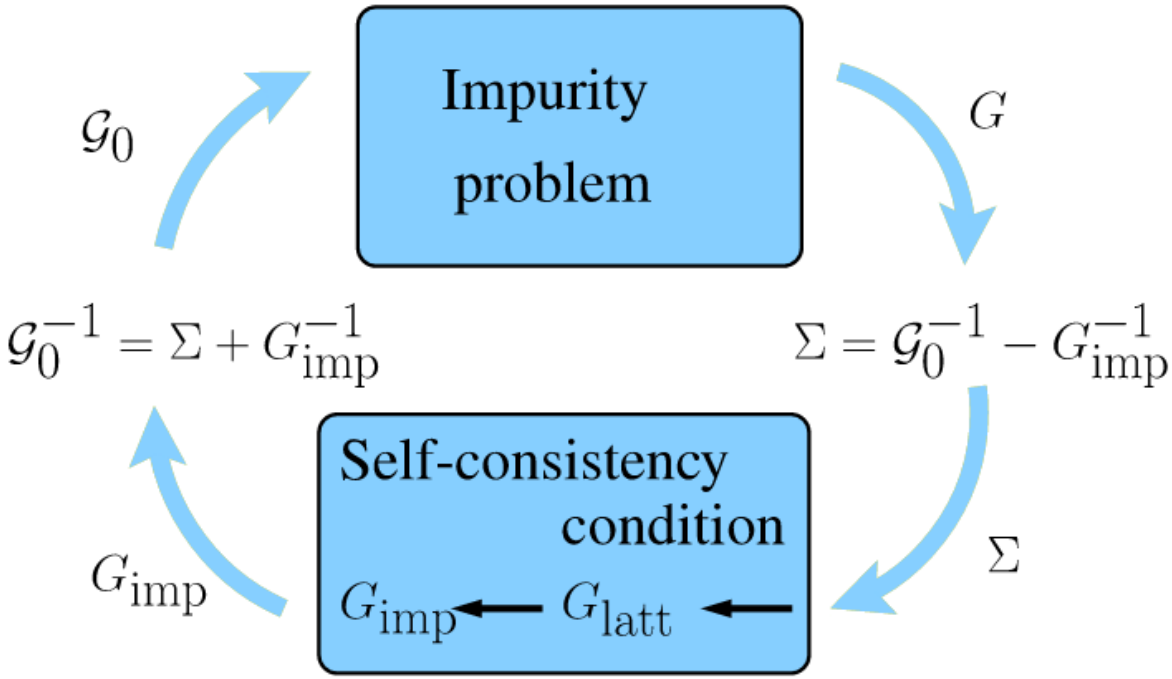

Figure 3: DMFT iterative loop

source: B. Amadon, Journal of Physics: Condensed Matter, Volume 24, Number 7

Real Time Impurity Solver

Pertubative expansion.

Single-orbital Anderson impurity model

$$H_{\text{imp}} = H_{\text{loc}} + H_{\text{bath}} + H_{\text{hyb}}$$

$$H_{\text{loc}} = \sum_{\sigma \in \uparrow,\downarrow} \varepsilon_\sigma d_\sigma^\dagger d_\sigma + U n_\uparrow n_\downarrow$$

$$H_{\text{bath}} = \sum_{\sigma,\lambda} \varepsilon_\lambda b_\lambda^\dagger b_\lambda$$

$$H_{\text{hyb}} = \sum_{\sigma,\lambda} (t_{\sigma\lambda} b_\lambda^\dagger d_\sigma + t_{\sigma\lambda}^* d_\sigma^\dagger b_\lambda)$$

- Write impurity Hamiltonian as a sum $H_{\text{imp}} = H_0 + H_{\text{int}}$
- Exact time evolution for H_0, pertubative expansion for H_{int}

Real Time Impurity Solver

Calculation of expectation values.

- Goal is to evaluate objects like $G^{<}(t,t') = i\langle d^{\dagger}(t')d(t)\rangle$ and $G^{>}(t,t') = -i\langle d(t)d^{\dagger}(t')\rangle$
- Expectation values are given by $\langle O(t)\rangle = Tr\left(\rho U^{\dagger}(t)\hat{O}U(t)\right)$
- Interaction picture propagator $U(t) = \exp^{iH_0 t}\exp^{-iHt}$ and operator $\hat{O}(t) = \exp^{iH_0 t}O\exp^{-iH_0 t}$
- Reduced Hamiltonian $H_0 = H_{\text{imp}} - H_{\text{hyb}}$

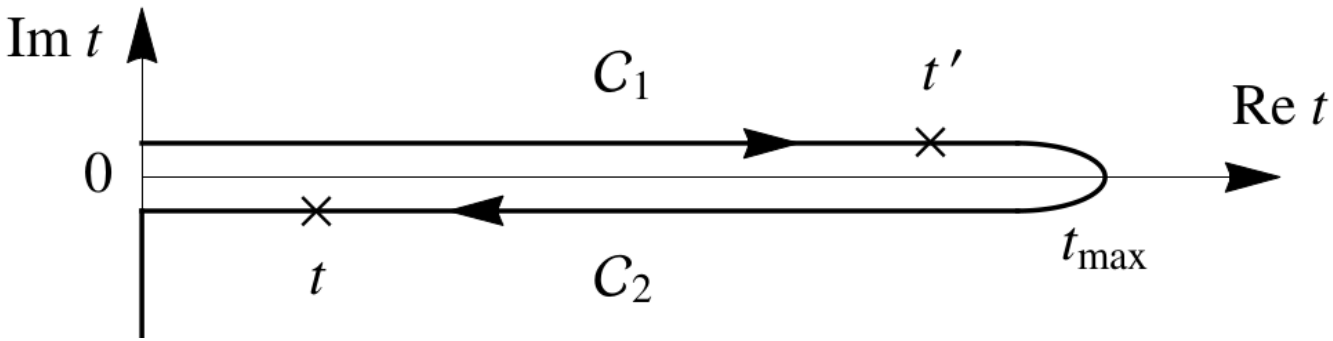

Figure 4: Keldysh Contour

source: H. Aoki, N. Tsuji, M. Eckstein, M. Kollar, T. Oka, and P. Werner, Rev. Mod. Phys. 86, 779 (2014)

Real Time Impurity Solver

Hybridization expansion.

- Expansion of $U(t)$ and $U^{\dagger}(t)$ in terms of $\widehat{H}_{\mathrm{hyb}}$:

$$U(t) = \sum_{n=0}^{\infty} (-i)^n \int_0^t dt_1 \int_0^{t_1} dt_2 \cdots \int_0^{t_{n-1}} dt_n \widehat{H}_{hyb}(t_1)\widehat{H}_{hyb}(t_2)\cdots\widehat{H}_{hyb}(t_n)$$

- Insert expansion for U(t) into propagator between many body states:

$$G(t) = \langle\langle \alpha \mid \rho_D exp^{-iHt} \mid \beta \rangle\rangle_B = \langle\langle \alpha \mid \rho_D \exp^{-iH_0 t}\, U(t) \mid \beta \rangle\rangle_B$$

- many body states are $|0\rangle, |\uparrow\rangle, |\downarrow\rangle, |\uparrow\downarrow\rangle$
- $\langle \cdots \rangle_B = Tr\{\rho_B \cdots\}$

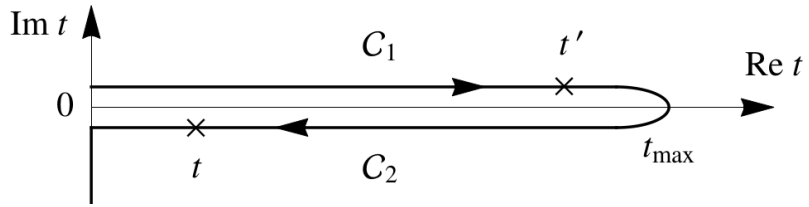

Figure 5: Keldysh Contour

Real Time Impurity Solver

Hybridization expansion.

$$G_{\alpha\alpha}(t) = G^{(0)}_{\alpha\alpha}(t) - \sum_{\gamma\delta}\int_0^t dt_1 \int_0^{t_1} dt_2\, G^{(0)}_{\alpha\alpha}(t-t_1) G^{(0)}_{\beta\beta}(t_1-t_2)\Delta^{\gamma\delta}_{\alpha\beta}(t_1-t_2) G^{0}_{\alpha\alpha}(t_2) - \cdots$$

with bare propagators

$$G^{(0)}_{\alpha\alpha}(t) = \langle\langle \alpha \mid \rho_D \exp^{-iH_0 t} \mid \alpha\rangle\rangle_B = \exp^{-i\varepsilon_\alpha t}$$

and Hybridization

$$\Delta(t_1-t_2) = \langle\alpha \mid d_\sigma \mid \beta\rangle\langle\beta \mid d^\dagger_\sigma \mid \alpha\rangle\Delta^{<}(t_1-t_2) + \langle\alpha \mid d^\dagger_\sigma \mid \beta\rangle\langle\beta \mid d_\sigma \mid \alpha\rangle\Delta^{>}(t_1-t_2)$$

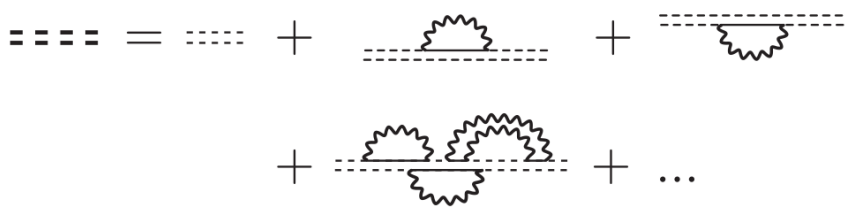

Figure 6: Example of diagrammatic expansion for bold propagators

Real Time Impurity Solver

Hybridization expansion.

Dyson equation

$$G_{\alpha\alpha}(t) = G^{(0)}_{\alpha\alpha}(t) + \int_0^t dt_1 \int_0^{t_1} dt_2\, G^{(0)}_{\alpha\alpha}(t - t_1)\Sigma_{\alpha\alpha}(t_1 - t_2)G_{\alpha\alpha}(t_2)$$

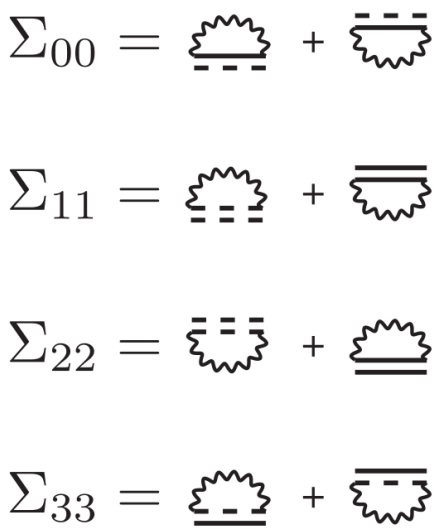

Self-consistent solution

1. Initialize $G_{\alpha\alpha}(t)$ with $G^{(0)}_{\alpha\alpha}(t)$
2. Compute self-energy $\Sigma_{\alpha\alpha}$(t)
3. Update $G_{\alpha\alpha}(t)$
4. go back to step 2

Figure 7: NCA Self-energy

source: G. Cohen, D. R. Reichman, A. J. M. and E. Gull; Phys. Rev. B89, 112139(2014)

Real Time Impurity Solver

Hybridization expansion.

Vertex functions

$$K_{\alpha\beta}(t,t') = K^{(0)}_{\alpha\beta}(t,t') + \sum_{\gamma\delta}\int_0^t dt_1 \int_0^{t'} dt_2 K_{\alpha\gamma}(t_1,t_2)\Delta_{\gamma\delta}(t_1,t_2)G^{\dagger}_{\delta\beta}(t-t_1)G_{\delta\beta}(t'-t_2)$$

$$K^{(0)}_{\alpha\beta}(t,t') = G^{\dagger}_{\alpha\beta}(t)G_{\alpha\beta}(t')$$

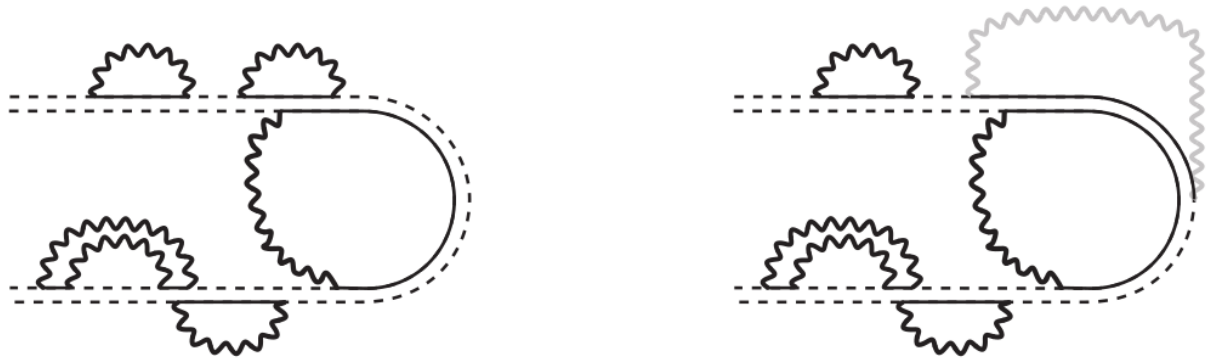

Figure 8: Diagrammatic expansion for Vertex functions

source: G. Cohen, D. R. Reichman, A. J. M. and E. Gull; Phys. Rev. B89, 112139(2014)

System

Bethe lattice in the initial Neel state.

Self-consistency condition

$$\Delta_{A(B),\sigma}(t,t') = v(t) G_{B(A),\sigma}(t,t') v^*(t')$$

Time-dependent electric field

$$H_{\mathrm{drv}}(t) = \sum_j eaE_0 sin(\omega t) s_j n_j$$

$$v_{ij}(t) = v_{ij} \exp^{iA(s_i - s_j)cos(\omega t)}$$

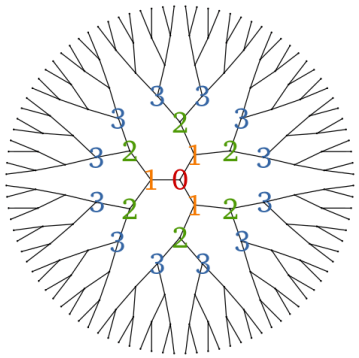

Figure 9: Structure of the Bethe lattice

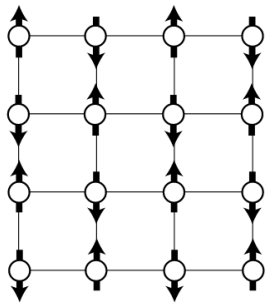

Figure 10: Classical anti-ferromagnetical Néel-state

Open systems

Free-fermion bath

$$H_{\text{tot}} = H_{\text{imp}} + H_{\text{fBath}} + H_{\text{fmix}}$$

$$H_{\text{fBath}} = \sum_{k,\sigma} \varepsilon_k f^{\dagger}_{k,\sigma} f_{k,\sigma}$$

$$H_{\text{fmix}} = \sum_{k,\sigma} (V_k f^{\dagger}_{k,\sigma} d_{\sigma} + V^{*}_{k} d^{\dagger}_{\sigma} f_{k,\sigma})$$

$$G(t,t') = (G_0^{-1}(t,t') - \Sigma_{fBath}(t,t') - \Sigma(t,t'))^{-1}$$

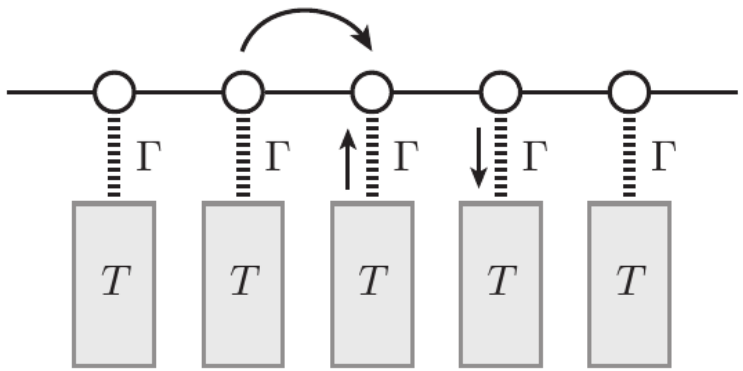

Figure 11: Schematic representation of a free-fermion bath model

Results

How does the ability to dissipate energy change in a non-equilibrium state?

$$I_E(t) = \langle \mathscr{I}_E(t) \rangle \text{ with } \mathscr{I}_E = \dot{H}_{\text{fBath}} = i \sum_{k,\sigma} \varepsilon_k \left(V_k d_\sigma f^\dagger_{k,\sigma} - V^*_k f_{k,\sigma} d^\dagger_\sigma \right)$$

$$P_\omega(A_{probe}) = \lim_{A_{probe} \to 0} \frac{dI_E(A_{probe}(\omega_{probe}))}{dA_{probe}(\omega_{probe})} \simeq \frac{I_E(\Delta A_{probe}(\omega_{probe}))}{\Delta A_{probe}(\omega_{probe})}$$

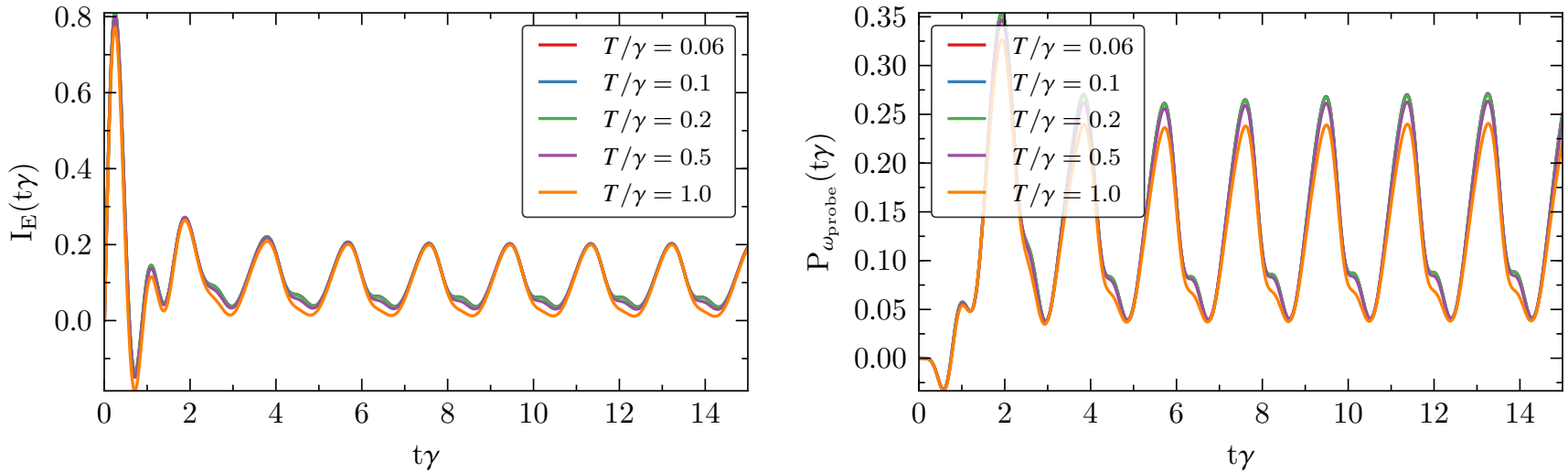

Figure 12: Example of heat current (left) and response (right) at resonant driving for a pump amplitude $\mathrm{A} = 1.0$ and a probe filed with parameters $\omega_{\text{probe}}/\gamma = 5$ and $\mathrm{A}_{\text{probe}} = 0.1$.

Results

Response of heat current at resonant driving.

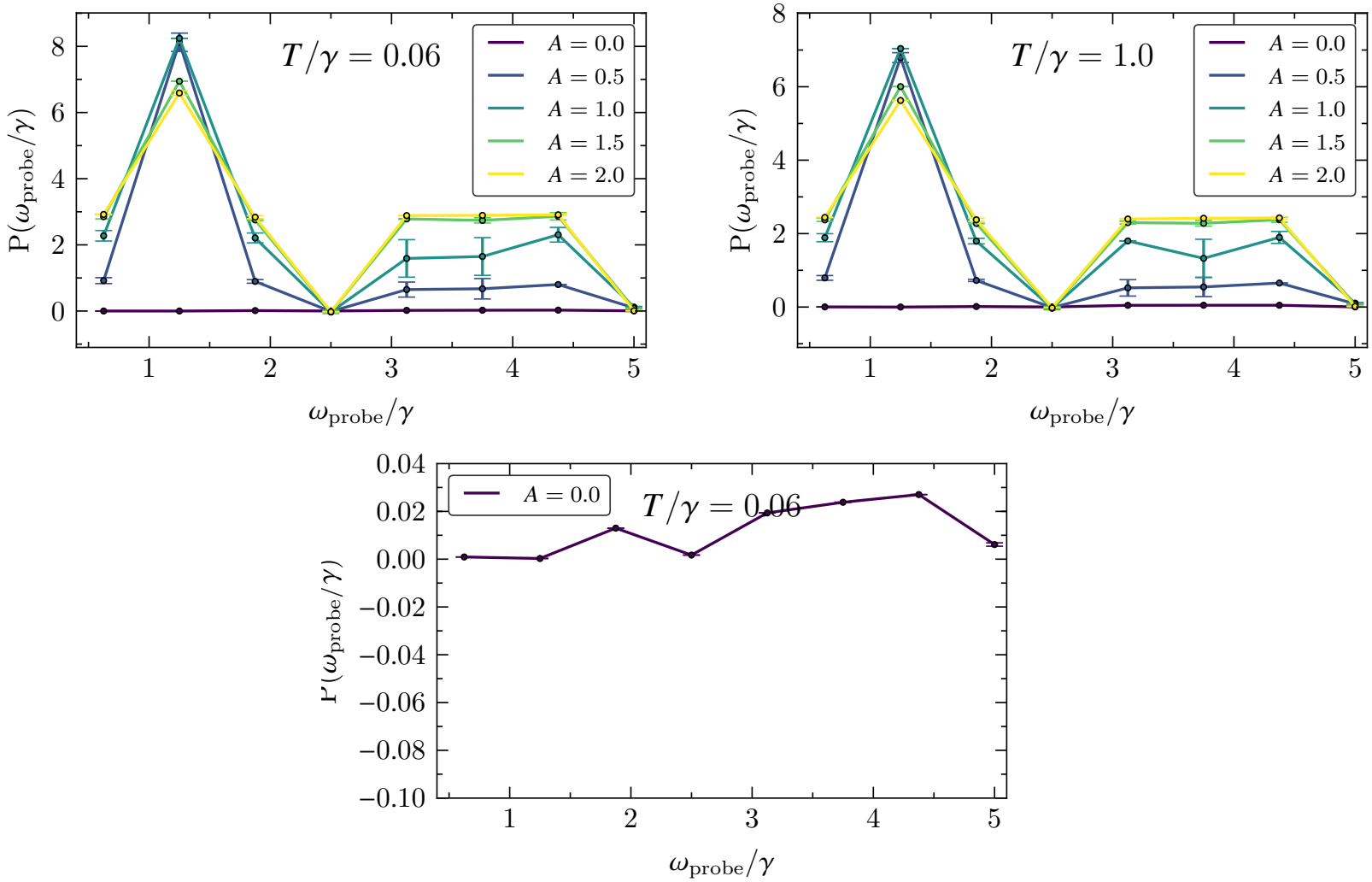

Figure 13: Average value of response $\mathrm{P}_{\omega_{\mathrm{probe}}}$ over a period T for various temperatures at resonant driving $\omega_{\mathrm{pump}}/\gamma = \mathrm{U}/\gamma = 5$.

Results

Response of heat current at resonant driving.

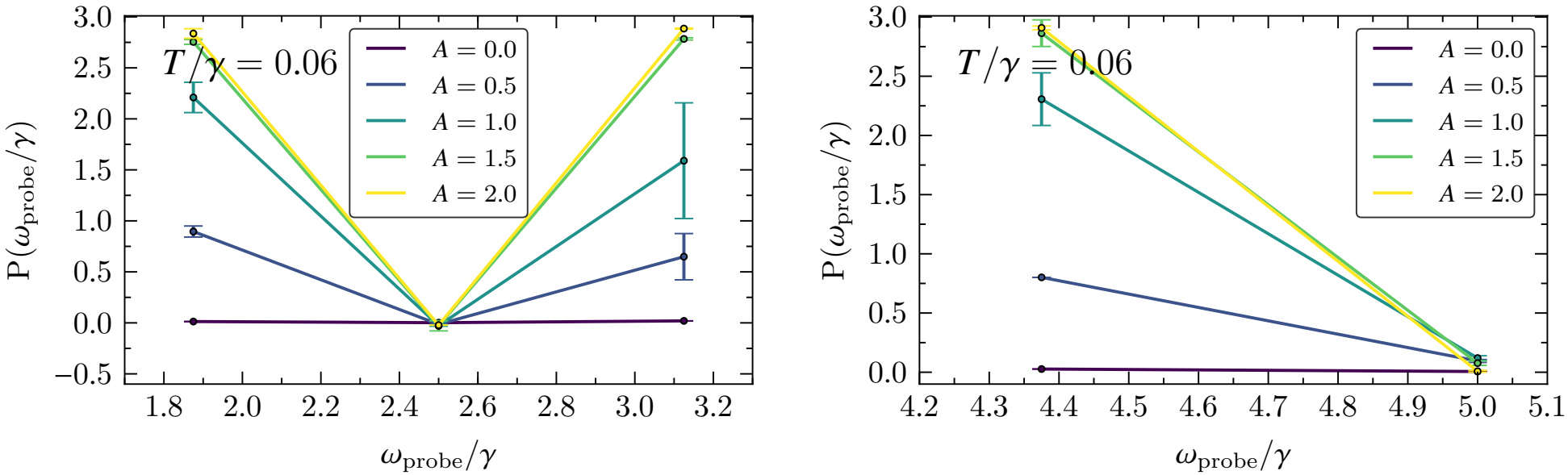

Figure 14: Zoom into $\omega_{\mathrm{probe}}/\gamma = 2.5$ and $\omega_{\mathrm{probe}}/\gamma = 5.0$

Results

Resonant pumping leads to an effective increase of the temperature.

$$A(\omega) = -\frac{1}{\pi} ImG^r(\omega) \text{ with } G^r(t,t') = \Theta(t-t')(G^>(t,t') - G^<(t,t'))$$

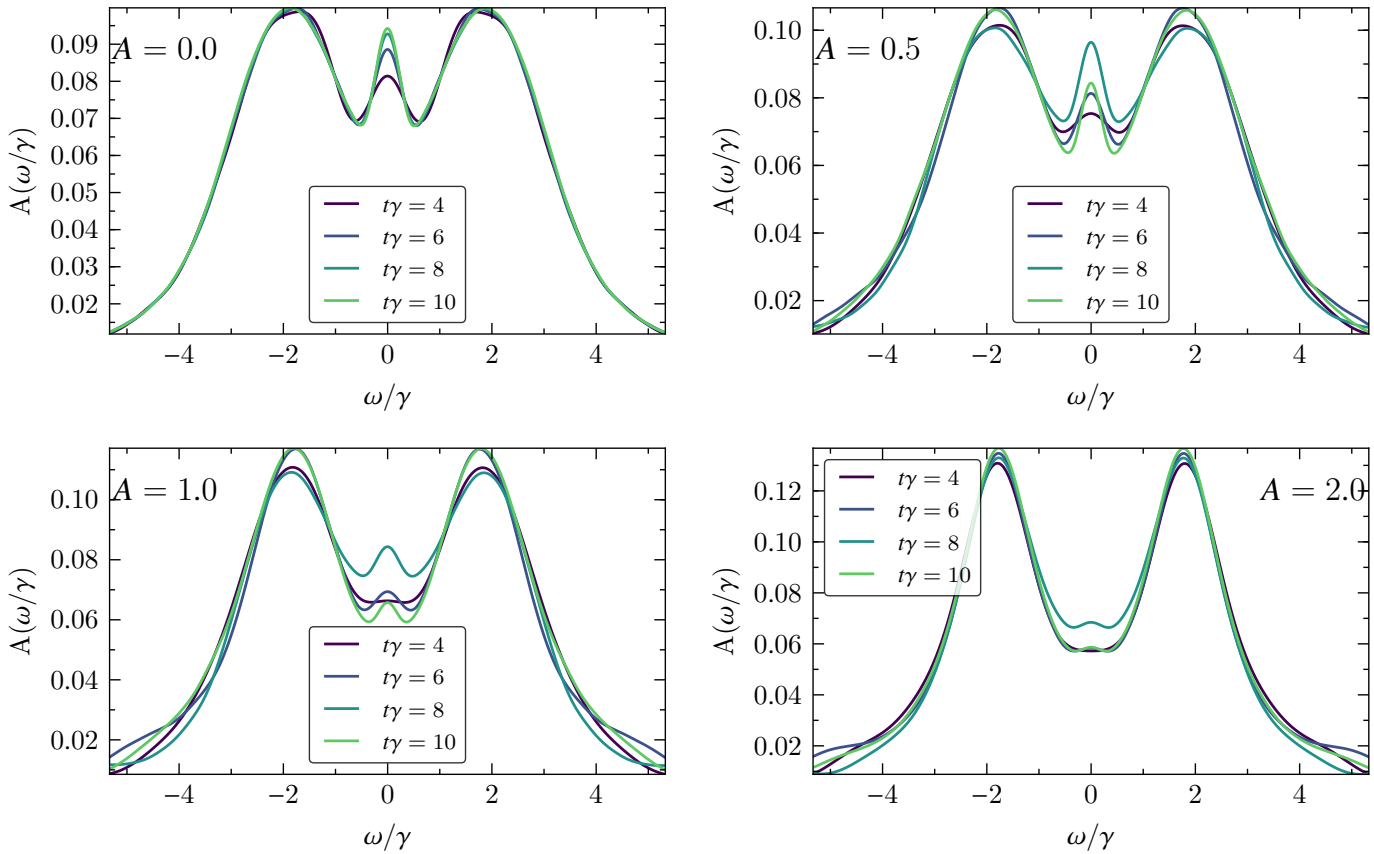

Figure 15: Time evolved spin-averaged spectral functions for various amplitudes at resonant driving and $T/\gamma = 0.06$.

Results

Increase of effective temperature and destruction of Kondo peak.

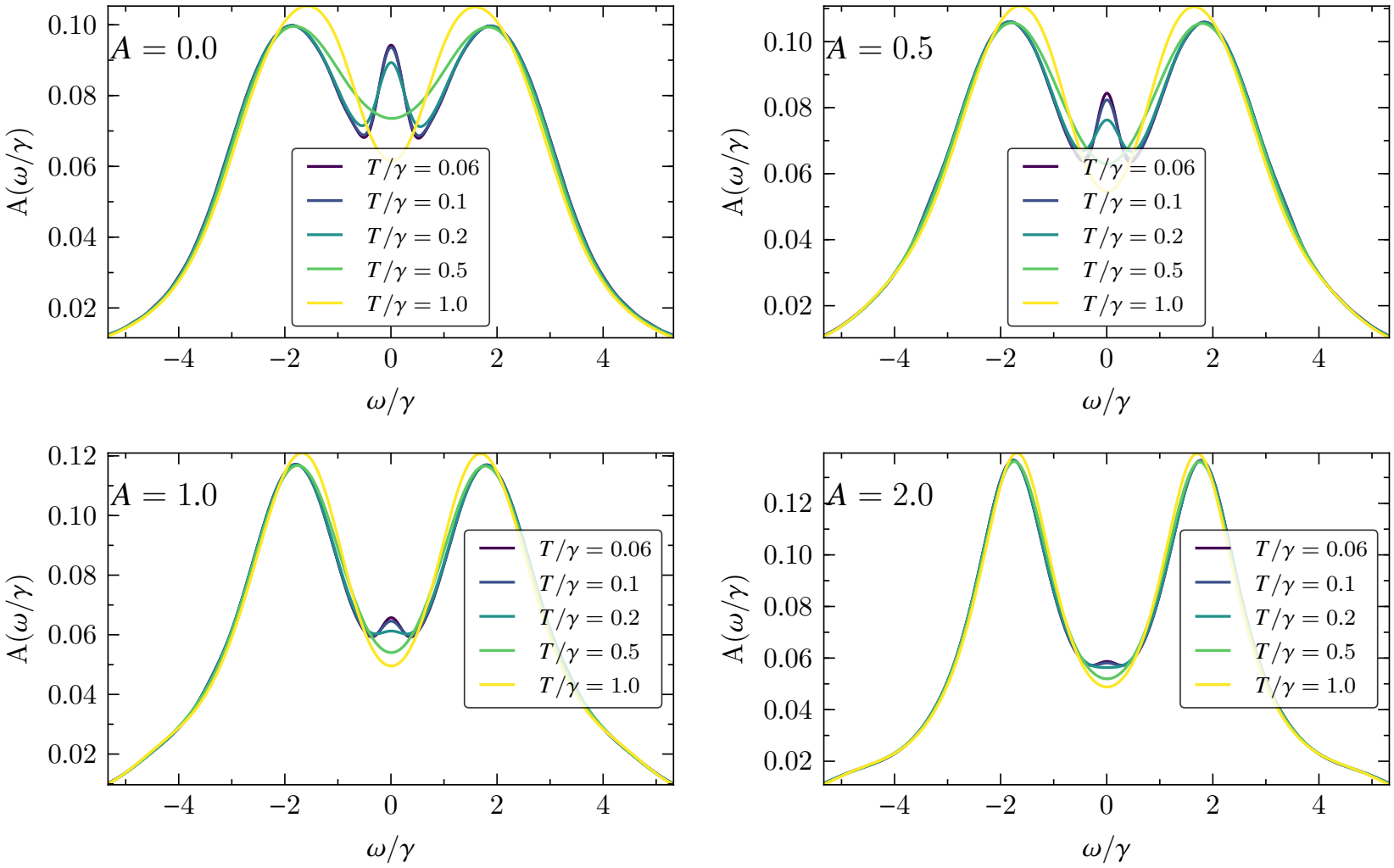

Figure 16: Steady-state spectral fuctions for various amplitudes at resonant driving $\omega_{\text{pump}}/\gamma = 5.0$.

Results

Response of heat current at half-resonant driving.

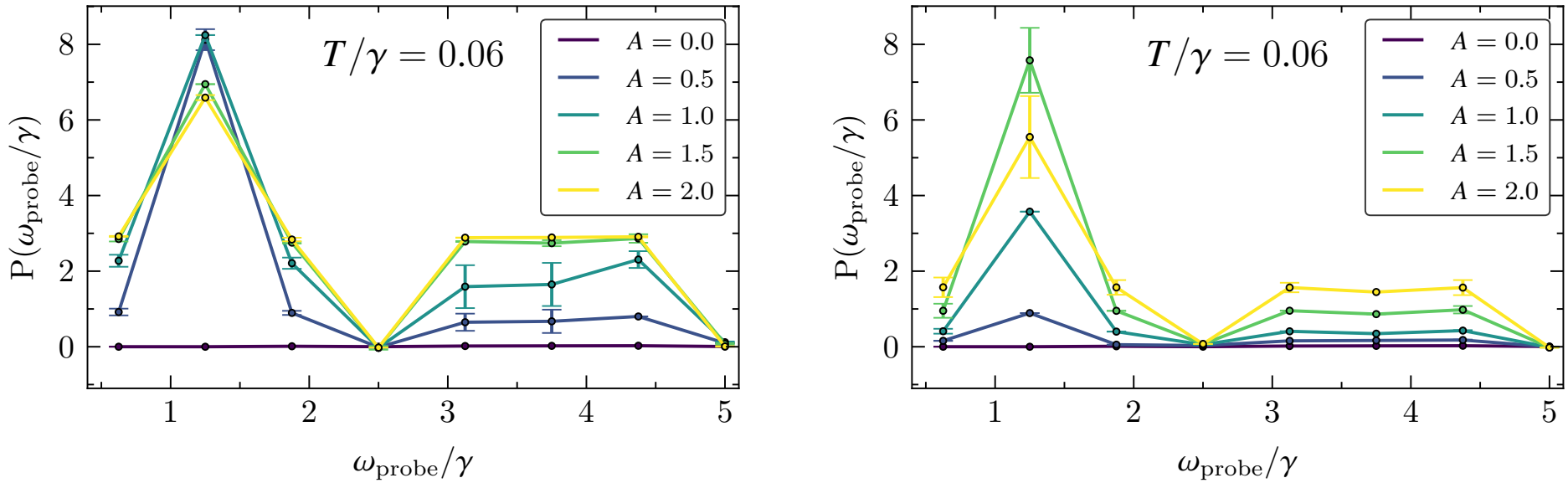

Figure 17: Comparison of resonant pumping with $\omega_{\mathrm{pump}}/\gamma = 5.0$ (left side) and half-resonant pumping with $\omega_{\mathrm{pump}}/\gamma = 2.5$ (right side).

Results

Response of heat current at half-resonant driving.

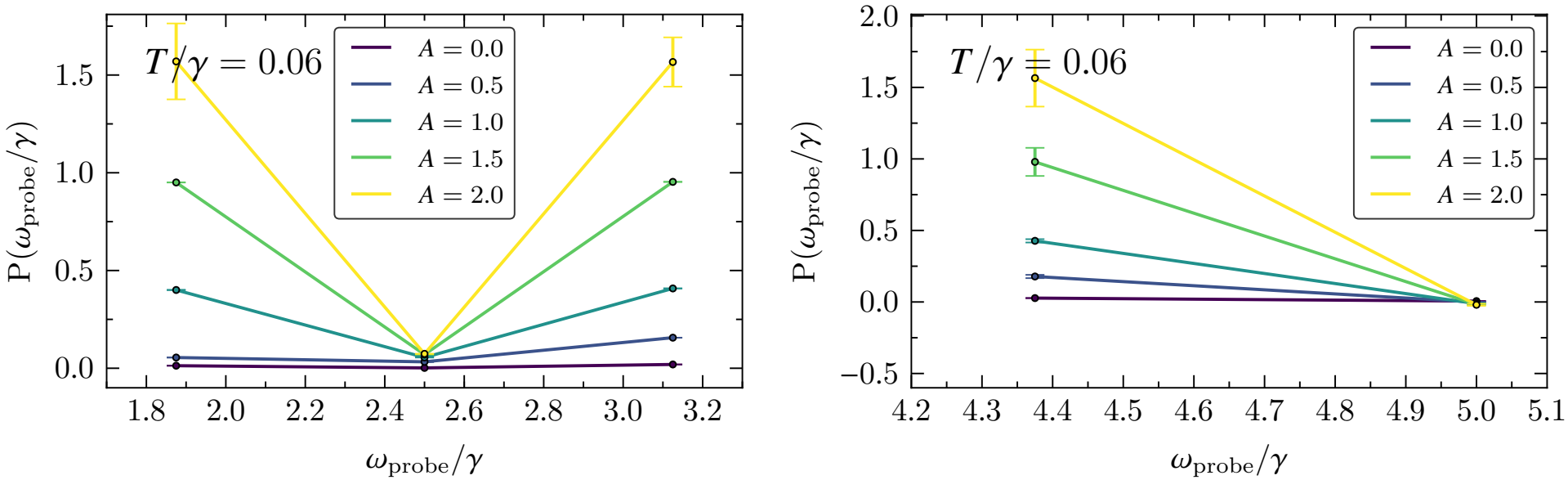

Figure 18: Zoom into $\omega_{\mathrm{probe}}/\gamma = 2.5$ and $\omega_{\mathrm{probe}}/\gamma = 5.0$

Results

Enhancement of Kondo physics even for temperatures above $T_k/\gamma = 0.17$ at half-resonant driving.

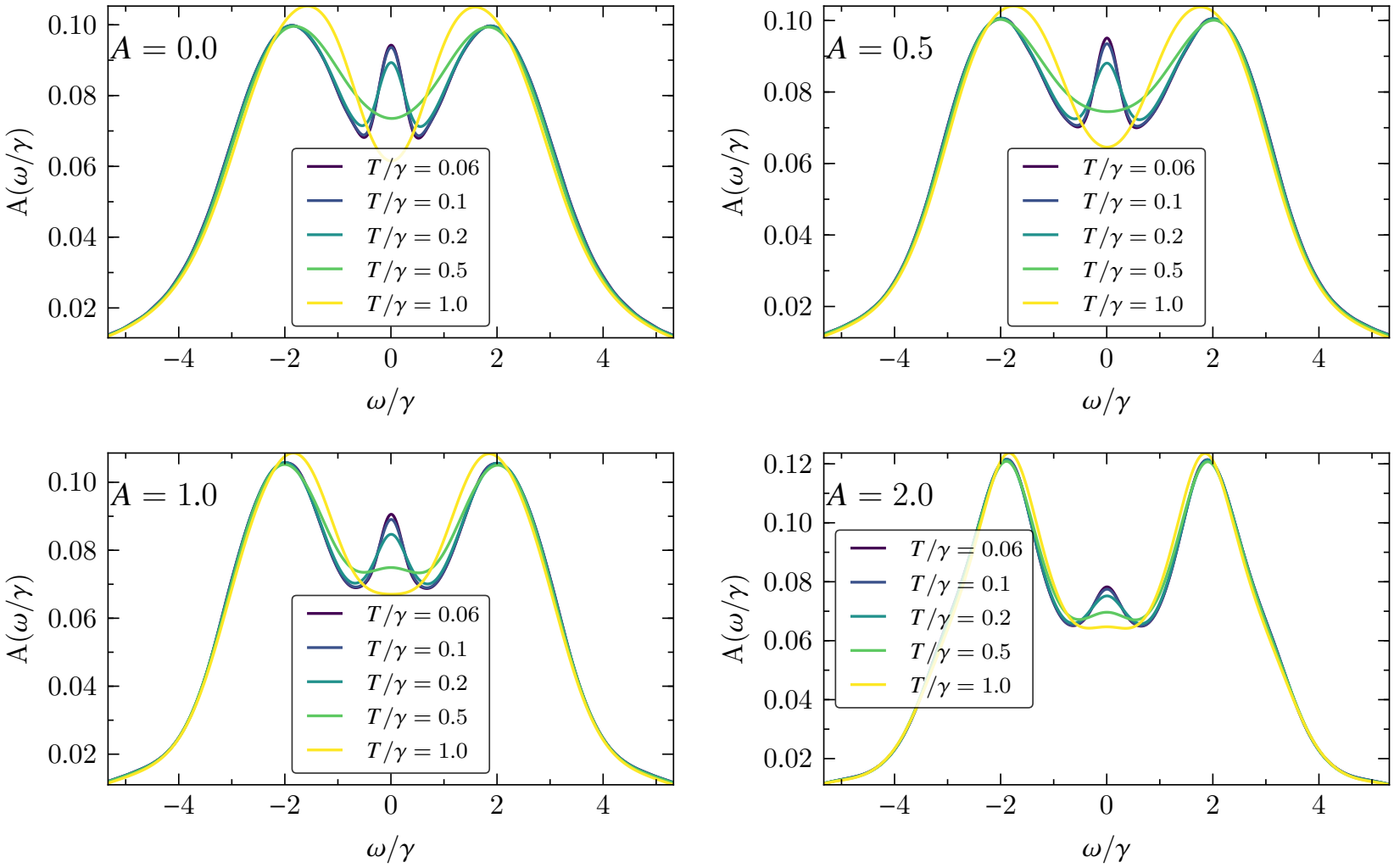

Figure 19: Spectral functions averaged over initial spin up and spin down state for various amplitudes at half-resonant driving $\omega_{\text{pump}}/\gamma = 2.5$.

Results

Comparison of response at resonant and half-resonant driving.

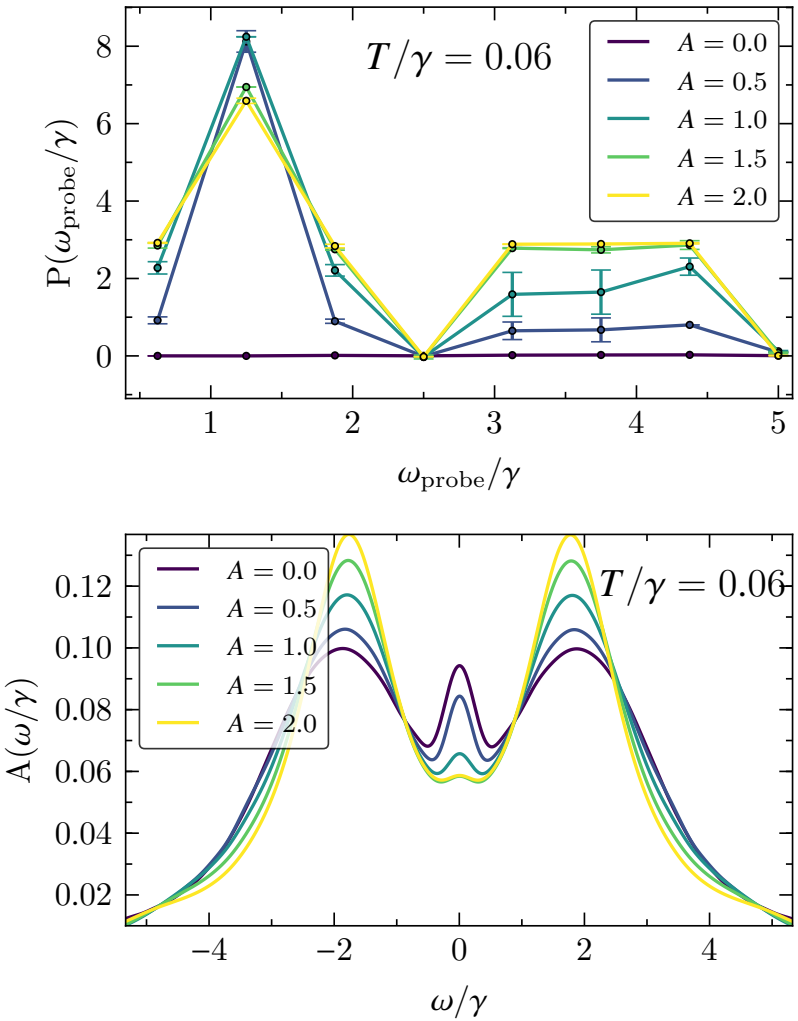

Figure 20: Response and spectral function at resonant driving $\omega_{pump}/\gamma = 5.0$.

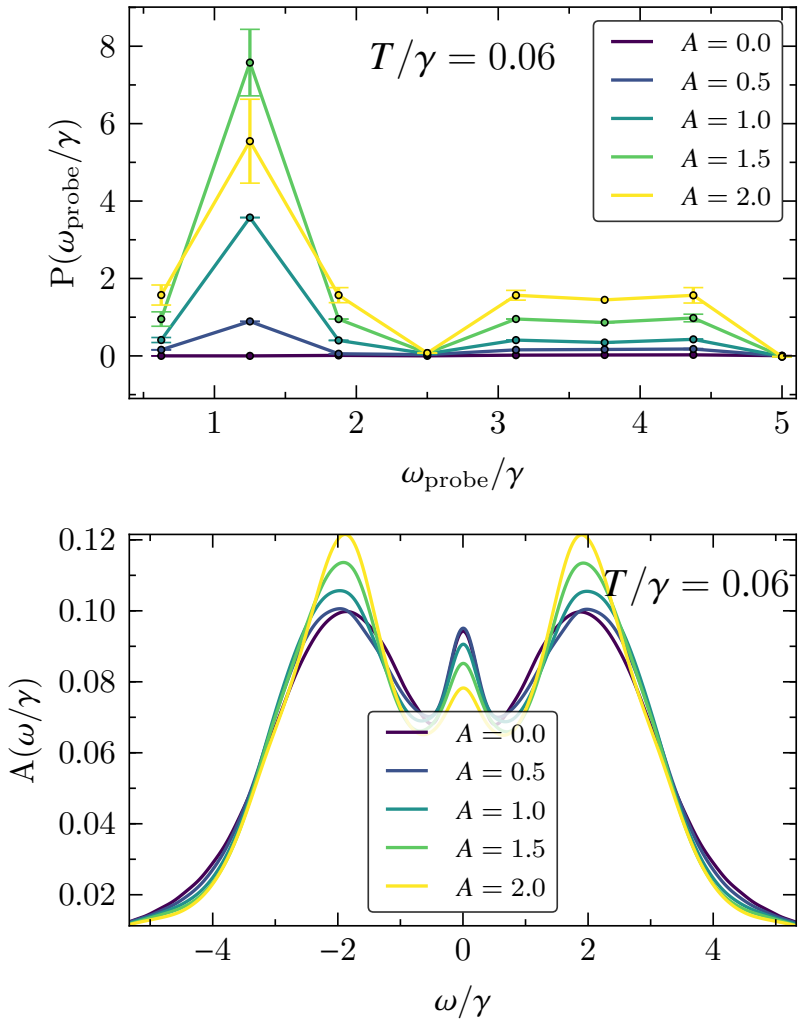

Figure 21: Response and spectral function at half-resonant driving $\omega_{pump}/\gamma = 2.5$.

Energy current

$$I_E(t) = \int_0^t d\tau \Delta_f^<(t,\tau) G^<(t,\tau)$$

$$\Delta_f^<(t,\tau) = \int_{-\infty}^{\infty} \frac{d\omega}{\pi} exp^{-i\omega(t-\tau)} \omega \Gamma(\omega) f(\omega - \mu)$$